DALTON
FULL PAPER

An X-ray absorption spectroscopic study at the mercury L_{III} edge on phenylmercury(II) oxygen species

Wendy J. Jackson,[a] Arild Moen,[b] Brian K. Nicholson,*[a] David G. Nicholson*[b] and Keith A. Porter[a]

[a] *Department of Chemistry, University of Waikato, Private Bag 3105, Hamilton, New Zealand*
[b] *Department of Chemistry, Norwegian University of Science and Technology, N-7491, Trondheim, Norway*

Received 20th August 1999, Accepted 10th December 1999

The X-ray absorption spectra of the reference and model compounds $HgCl_2$, PhHgCl, PhHgOAc and $[(PhHg)_2OH][BF_4]\cdot H_2O$ have been analysed in both the XANES and EXAFS regions, and the technique was extended to determine the structures of $(PhHg)_2O$, PhHgOH, and the basic salts $PhHgOH\cdot PhHgNO_3$ and $PhHgOH\cdot(PhHg)_2SO_4$, which were previously structurally uncharacterised. Results indicate that $(PhHg)_2O$ is a molecular species with Hg–O–Hg 135°, while PhHgOH contains the $[(PhHg)_2OH]^+$ cation and is better formulated as $[(PhHg)_2OH]OH$. The same cation is also featured in the two basic salts. Electrospray mass spectral studies of PhHgOH in aqueous solutions show that $[PhHgOH_2]^+$, $[(PhHg)_2OH]^+$ and $[(PhHg)_3O]^+$ co-exist in solution in a pH-dependent equilibrium.

Introduction

Grdenic and Zado showed many years ago that "methyl mercury hydroxide" does not exist as such, but is better formulated as $[(MeHg)_3O]OH$, containing the tris(methylmercurio)oxonium cation.[1] This cation has been characterised crystallographically as the $[ClO_4]^-$ and $[NO_3]^-$ salts,[2] showing a flattened pyramidal Hg_3O core, with Hg–O–Hg angles of 116°. In aqueous solutions of "MeHgOH" spectroscopic evidence suggests that the species $[MeHgOH_2]^+$, $[(MeHg)_2OH]^+$ and $[(MeHg)_3O]^+$ are all present in a pH-dependent equilibrium, but only the last of these cations has been isolated.[1,3] Related cations which have been characterised[4] include $[(ClHg)_3O]^+$, $[(MeHg)_3S]^+$ and $[(MeHg)_3Se]^+$.

For the corresponding aryl mercury system there is less information. Bloodworth reports a true PhHgOH, which is dehydrated to a stable $(PhHg)_2O$, based on spectroscopic and gravimetric data.[5] More recently Doring *et al.* have demonstrated that $Ni(acac)_2$ catalyses the disproportionation reaction of PhHgOH to Ph_2Hg, HgO and H_2O, and they isolated a dimeric nickel complex with a bridging $(PhHg)_2O$ ligand which may be an intermediate in the process.[6]

On the other hand Green[7] assigns up to three IR bands as Hg–O stretches for the material known as PhHgOH, which is inconsistent with isolated molecules, so the true nature of PhHgOH is still unknown. Similarly the actual forms of the long-known "basic phenyl mercury salts" $(PhHgOH\cdot PhHgX)$ $(X = NO_3^-, BF_4^-, CO_3^{2-}, SO_4^{2-}$ *etc.*) are not well established. In an earlier X-ray crystallographic study we showed that the basic tetrafluoroborate contained the $[(PhHg)_2OH]^+$ cation[8] and Grdenic found the same species in a related nitrate.[9] No evidence for the tris(phenylmercurio)oxonium cation, corresponding to the methyl analogue, was found in these earlier studies. Characterisation of these species by X-ray diffraction has so far been limited by the difficulty in obtaining suitable single crystals. The compounds generally form as powders or extremely thin crystals.

We now report the results of an X-ray absorption spectroscopy examination of PhHgOH and of some basic phenyl mercury salts, together with suitable model compounds. Previous Hg XAS publications include a study of the structure and solvation of HgX_2 (X = Cl, Br, CN),[10] and an examination of intercalation of HgX_2 in high-T_c superconducting lattices;[11] these provide a useful basis for the interpretation of the present results. We also describe electrospray mass spectrometric (ESMS) examination of aqueous solutions of PhHgOH at different pH's.

Experimental

The compounds PhHgOH, $(PhHg)_2O$, $PhHgOH\cdot PhHgNO_3$ and $PhHgOH\cdot(PhHg)_2SO_4$ were prepared as described in the literature.[5,7,8,12] An improved synthesis of $[(PhHg)_2OH][BF_4]\cdot H_2O$ is given below (*cf.* ref. 8). Other compounds were commercially available. Purity of PhHgOH,[5] $(PhHg)_2O$[5] and of the basic nitrate[7] was confirmed by comparison of melting point behaviour and IR spectra with those in the literature. The basic sulfate was prepared using the method of Barlow and Davidson[12] and had a matching IR spectrum. However the melting point found in the present study (152–158 °C) differed markedly from the literature value (270–280 °C) so microanalysis was used to confirm the formulation (found: C 22.9, H 1.9, S 3.2%, $C_{18}H_{16}Hg_3O_5S$ requires C 22.9, H 1.7, S 3.4%).

Electrospray mass spectra were recorded on a VG Platform II quadrupole mass spectrometer using H_2O or H_2O–MeCN (1 : 1) as a mobile phase at 0.01 mL min^{-1}. The sample was dissolved in a small amount of the solvent and the pH was adjusted by adding NaOH or HNO_3 solutions. Assignment of peaks was confirmed by simulation using the *Isotope* program.[13]

Improved synthesis of $[(PhHg)_2OH][BF_4]\cdot H_2O$

PhHgOH (1.0 g, 3.4 mmol) was added to H_2O (35 mL) in a beaker. The mixture was heated to 100 °C to form a homogeneous solution. Aqueous HBF_4 (0.36 mL of 40%, 1.64 mmol) was added and the solution was left to cool. Clear needle-shaped crystals formed, were collected by filtration (0.50 g, 44%), and were identified by comparison of the X-ray diffraction pattern with that of an authentic sample.[8]

X-Ray absorption data collection

XAS data were collected using the facilities of the Daresbury Laboratory SRS, UK, and the Swiss-Norwegian Beamline (SNBL) at the European Synchrotron Radiation Facility (ESRF), Grenoble, France. Spectra were measured at the mercury L_{III}-edge ($\lambda = 1.0094$ Å; energy = 12 282 eV) in the transmission mode on stations 7.1 (Daresbury) and EH1 (SNBL-ESRF).

At Daresbury the average beam current was 200 mA at 2.0 GeV. Station 7.1 is equipped with an order-sorting silicon(111) monochromator that was offset to 50% of the rocking curve for harmonic rejection. An unfocussed beam of dimensions 0.8 mm vertically and 10 mm horizontally was used. Gas ion chambers were used to detect the intensities of the incident and transmitted X-rays. The first ion chamber was filled with Ar at partial pressure 156 Torr and the second ion chamber with Xe at atmospheric pressure. These gases account for 20% and 80% absorption, respectively.

At the SNBL a channel-cut silicon (111) monochromator with an unfocussed beam was used to scan the X-ray spectra. The beam currents ranged from 80–130 mA at 6.0 GeV. Higher-order harmonics (*ca.* two orders of magnitude) were rejected by means of a gold-coated mirror from a beam of size 1.2 × 4.0 mm as defined by the slits in the station. The ion chamber gases were at ambient temperature and pressure and were as follows: detector length 17 cm, 18% Ar, 82% N_2 for I_0; length 31 cm, 83% Ar, 17% N_2 for I_t. The maximum resolution ($\Delta E/E$) of the Si(111) bandpass is 1.4×10^{-4}. Reproducibility in edge position was estimated to be *ca.* 0.15 eV.

For both stations room temperature mercury L_{III}-edge data ($E = 12\,282$ eV, $\lambda = 1.00944$ Å) were registered over the energy range 12 113–13 140 eV. In addition, spectra were measured over the pre-edge and XANES regions (12 113–13 325 eV with a step size of 0.25 eV over the edge and XANES region).

Energy calibrations were effected by regularly measuring the spectrum of $HgCl_2$ (thickness corresponding to 1.5 absorption lengths). This compound was chosen to be the reference because the energy of the first deflection (assigned to 12 282 eV) has been defined as the L_{III} edge.[10] Reference data were measured prior to each data collection because accurate calibrations are particularly important for the pre-edge and XANES regions where the need for comparisons between the different spectra makes it necessary to define the absolute energies of the spectral features. For the EXAFS the energy is relative to the individual edges which are therefore defined as zero. The XAS of $(PhHg)_2O$, PhHgOH, PhHgOH·$PhHgNO_3$ and PhHgOH·$(PhHg)_2SO_4$ and the reference and model compounds $HgCl_2$, PhHgCl, PhHgOAc and $[(PhHg)_2OH][BF_4]\cdot H_2O$ were measured. The amounts of material in the XAS samples were calculated from element mass fractions and the absorption coefficients of the constituent elements[14] just above the absorption edge to give an absorber thickness of 1.5 absorption lengths.

Spectra were measured on well-powdered samples intimately mixed with boron nitride to give a sample thickness of *ca.* 1.0 mm, placed in aluminium sample holders and sandwiched between Kapton windows. Four to six scans of each compound were collected and summed to give the final spectra.

EXAFS Data analysis

The data were corrected for dark currents, converted to *k*-space, summed and background subtracted to yield the EXAFS function $\chi^{obs}_i(k)$ using the EXCALIB and EXBACK programs.[15] Model fitting was carried out with EXCURV90 using curved-wave theory and *ab initio* phase shifts.[15] The edge positions were determined from the first inflection points of the derivative spectra. The phase shifts experienced by the photoelectron, the amplitude of the backscattering and the electron mean free path were calculated from within EXCURV90 using spherical wave theory and a single scattering model but with multiple scattering pathways for the phenylcarbon atoms and the Hg–O–Hg fragments. The spectra were Fourier transformed using phase-shifts calculated for the first atom shell to give the radial distribution function.

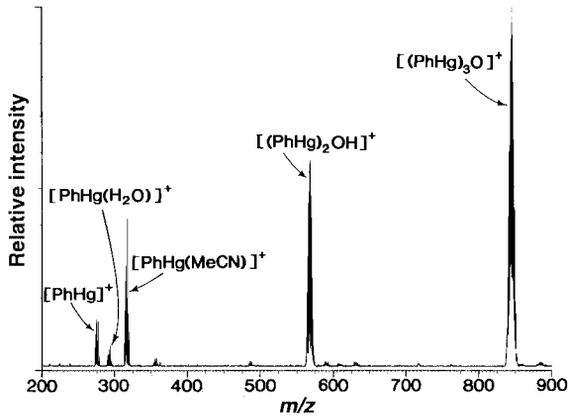

Fig. 1 The electrospray mass spectrum of a solution of PhHgOH in MeCN : H_2O (1 : 1) at pH *ca.* 7.

The known structures of the model compounds PhHgCl, PhHgOAc, and $[(PhHg)_2OH][BF_4]\cdot H_2O$ [refs. 8, 16, 17] were used to check the validity of the *ab initio* phase shifts and amplitudes for mercury, oxygen and carbon backscatterers and to establish the general parameters, AFAC (proportion of absorption causing EXAFS) and VPI (allows for inelastic scattering of the photoelectron).[15] During least squares fitting it is important to avoid correlation between the parameters which strongly affect the EXAFS amplitude and between those that influence the frequency of the EXAFS oscillations. Therefore, the EXAFS spectra were least squares fitted using k^1 and k^3 weighted data because, as has been shown,[18] optimising the k^1 and k^3 weighted fits reduces the degree of coupling between the two highly correlated sets of parameters (N, $AFAC$, $2\sigma^2$ and r, E_0) giving a solution common to both weighting schemes, where N is the multiplicity, $2\sigma^2$ the Debye–Waller type factor, r the distance and E_0 the magnitude of the photoelectron energy at zero wave vector). The values for AFAC and VPI used were 0.72 and −4.00, respectively.

The k^3 weighting scheme used in the refinement compensates for the diminishing photoelectron wave at higher k. The curve-fitting was performed on data that had been Fourier filtered over a wide range (1.0–25.0 Å). This filter removes low-frequency contributions to the EXAFS below 1 Å, but does not smooth the spectrum (*i.e.* the noise is not removed). This procedure must not be used to correct for unsatisfactory background subtraction. All of the spectra were treated in exactly the same manner and the validity of the data reduction and fitting procedures was checked against the spectra of the reference compounds. The data were analysed over the range $k = 3.0$–14.0 Å^{-1}, and the refinement carried out to minimise the fit index (FI):

$$\mathrm{FI} = \sum_i [k^3(\chi_i^{exp} - \chi_i^{calc})]^2$$

where χ_i^{exp} and χ_i^{calc} are the experimental and theoretical EXAFS respectively.[15]

Results and discussion

Electrospray mass spectrometry

Aqueous solutions of PhHgOH gave three main signals in the positive ion mass spectra, depending on pH, see Fig. 1. Under acid conditions (*ca.* pH 2) the dominant signal was centred about *m/z* 297 and was assigned to the species $[PhHgOH_2]^+$, which can be regarded as either protonated PhHgOH or

solvated $PhHg^+$. At higher skimmer cone voltages, where fragmentation is expected, the unsolvated species $PhHg^+$ at *m*/*z* 279 was increasingly evident.

As the pH increased towards neutral a signal corresponding to the $[(PhHg)_2OH]^+$ ion at *m*/*z* 573 became apparent, while at pH 10 the dominant species was the previously unknown $[(PhHg)_3O]^+$ cation at *m*/*z* 849. This last ion was very stable towards fragmentation in the mass spectrometer even under quite harsh conditions.

Essentially the same results were obtained in H_2O–MeCN (1:1) except that under acid conditions the ions $[PhHg(NCMe)]^+$ at *m*/*z* 321 dominated over $[PhHgOH_2]^+$ suggesting that the $PhHg^+$ cation has a greater affinity for the N-donor solvent molecules.

These ESMS results clearly show that the equilibria established much earlier for the $MeHg^+$ system[3] have direct parallels with the $PhHg^+$ system and that, in particular, the $[(PhHg)_3O]^+$ ion is quite stable. It must therefore also be considered along with $PhHg^+$ and $[(PhHg)_2OH]^+$ as a possible contributor to solid state structures, even though it has not yet been structurally characterised.

X-Ray absorption spectroscopy

Depending on the element, the pre-edge region of an X-ray absorption spectrum sometimes contains features of structural or electronic interest. Thus, features close to the absorption edge often can be assigned to electronic transitions from 1s or 2p orbitals (K- or L-edges, respectively) to higher bound states, the energies of which lie within the discrete part of the spectrum and give information about the valence state of the absorbing atom and its geometry. The edge itself defines the threshold ionisation energy, above which lies the continuum with oscillations (XANES and EXAFS) superimposed on a smoothly varying background of photoelectron energy. These oscillations, or fine structure, reflect the electronic and geometric characteristics of the molecular environment of the chosen atom. In this paper, we use the discrete part of the spectra (pre-edge features) to establish the local geometry about the mercury(II) atoms, and the EXAFS region to extract distances.

The present study examined three compounds of known structure ($HgCl_2$, PhHgCl and PhHgOAc) to provide a series leading from the previously examined[10] $HgCl_2$ to a sample with the C,O-coordination assumed for the rest of the samples. These served to validate the general analysis of the X-ray absorption spectra. The compound $[(PhHg)_2OH][BF_4]\cdot H_2O$ was used as a model for the remaining species of unknown structure, namely PhHgOH, $(PhHg)_2O$ and the basic nitrate and sulfate.

The XANES and their first derivatives

Fig. 2 shows the Hg L_{III}-edge XANES of the aryl mercury(II) compounds (including the model and reference compounds); also shown (Fig. 3) are the first derivatives of the XANES spectra.

Each of the XANES spectra exhibits an intense pre-edge peak at about 12283 eV. The high intensities of these peaks are consistent with an allowed electric–dipole transition. This, together with the energies, indicates that 2p→6s(Hg) and 2p→ ligand orbitals are possible assignments.[10,11] In the case of copper(I) compounds at the K-edge, the intensity of the pre-edge peak is connected to the 1s→4p transitions often observed for transition metal compounds.[19,20] With one notable exception, linear two-coordinate copper(I) compounds exhibit higher intensities than three- and four-coordinate systems.[21] Although the selection rules are different for K-edges it has been suggested that mercury(II) follows the same pattern, namely that the intensity of the 12 283 eV peak decreases in the order linear > tetrahedral > octahedral.[10,11]

From this it is evident that the high intensities of the pre-edge peaks of all of the present compounds are characteristic of

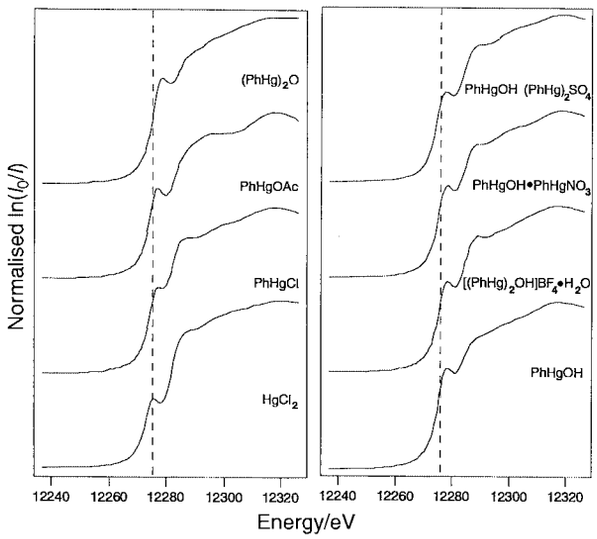

Fig. 2 Normalised Hg L_{III}-edge XANES of the samples and reference/model compounds.

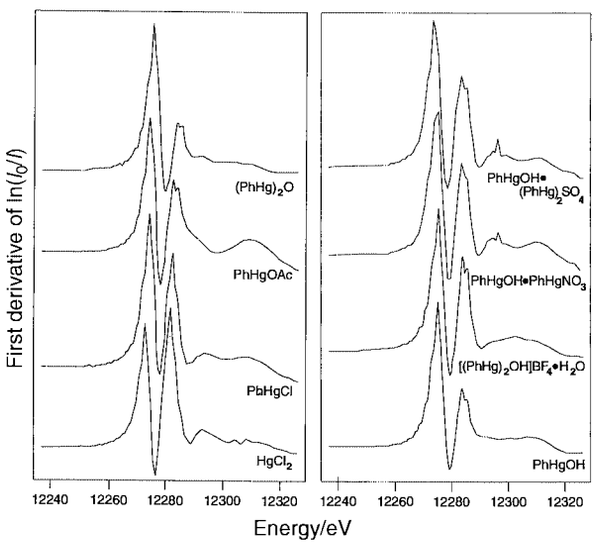

Fig. 3 The first derivatives of the XANES spectra for the samples and the reference/model compounds.

linearly coordinated mercury(II) atoms. The pre-edge peaks for the chlorine-containing compounds $HgCl_2$ and PhHgCl are at slightly lower energies than the corresponding peaks for the other compounds.

The first derivatives of the edge regions are useful for highlighting characteristic features (including any pre-edge features) and for more accurately establishing the transition energies.[22] The diagrams in Fig. 3 clearly show that the metal atoms in all of the aryl-mercury compounds are in very similar environments. The first-derivative spectra of $HgCl_2$ and of PhHgCl are quite symmetric but the C,O-bonded examples are less symmetrical and consistently show a small but significant splitting of the higher energy feature. Similar splitting has been previously noted for $Hg(CN)_2$, but no definite assignment was given.[10]

The data in this region are limited largely to confirming that all of the compounds examined contain linearly coordinated mercury(II), which is as expected. Nevertheless it probably precludes association of the type proposed for PhHgOMe or PhHgOEt where dimers **1** or trimers **2** with three-coordinate mercury(II) are implicated,[23] and which would be possible for PhHgOH or $(PhHg)_2O$ in particular. We note that the best model fitted to the EXAFS of $PhHgOH\cdot PhHgNO_3$ includes two weaker additional oxygen interactions which we assume

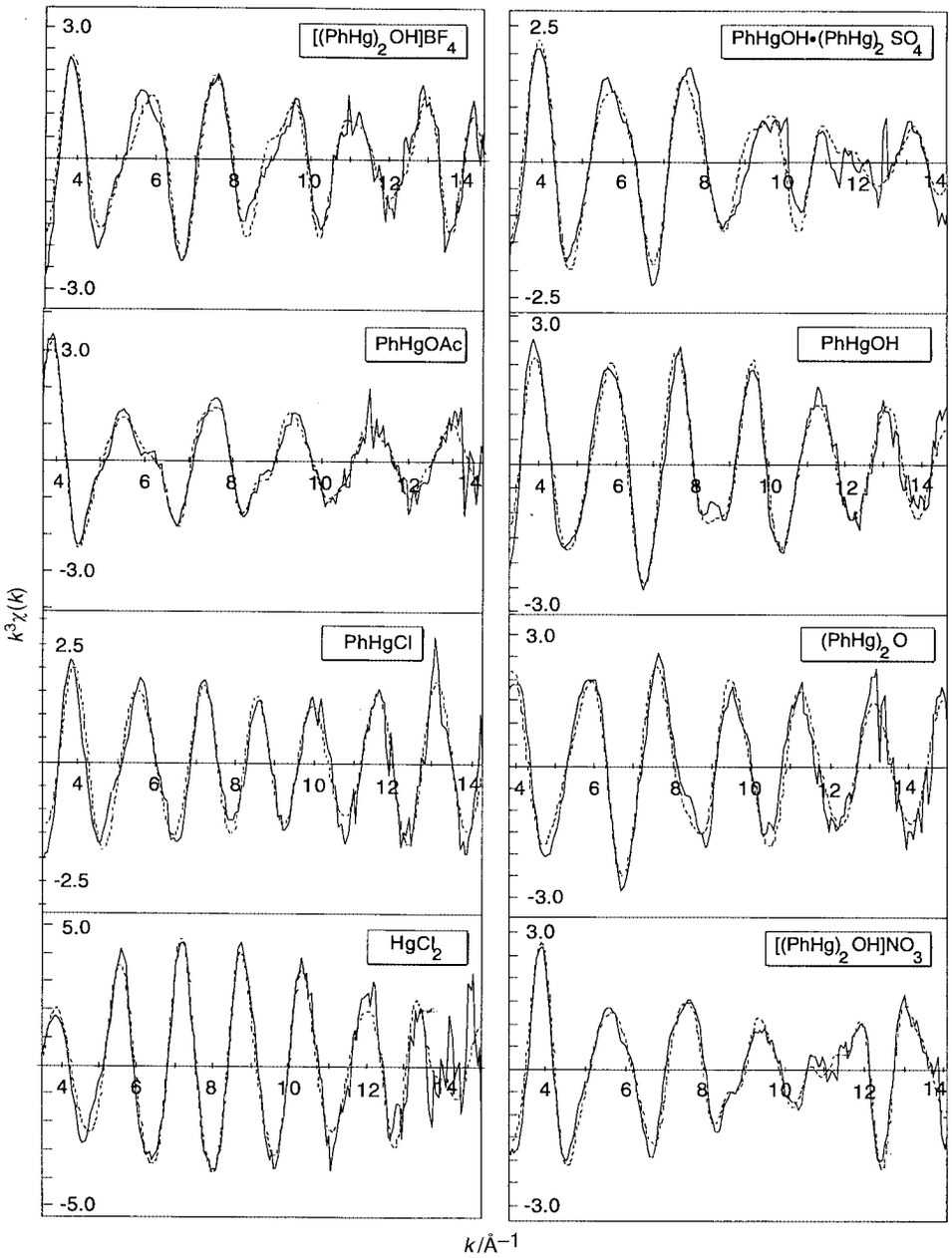

Fig. 4 k^3-Weighted experimental and least-squares fitted EXAFS of the samples and reference/model compounds. The solid line shows the experimental data and the broken line represents the calculated EXAFS (see Table 1).

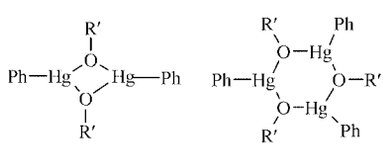

1 **2**

stem from the nitrate anion (see below). Similarly, consistent with its crystal structure, anion contacts (three F atoms from BF_4^-) were also found in the model for the basic salt $[(PhHg)_2OH][BF_4]\cdot H_2O$. However these longer range interactions do not seem to significantly affect the edge features.

EXAFS Analysis

It is essential to identify the maximum number of independent parameters, N_{ind}, that may be varied in the EXAFS analysis to give meaningful results. This is given by $N_{ind} = 2\Delta k\Delta R/\pi$ where Δk is the extent of the data in k-space and ΔR the range of distance being modelled.[24] For these analyses the maximum value corresponds to Δk = 3–14 Å $^{-1}$, ΔR = 2–4 Å and N_{ind} = 14. The number of parameters is reduced by making use of chemical knowledge. Thus the multiplicities of the neighbouring atoms (shells) of the mercury environments are known and therefore have been fixed so that the number of parameters varied is within this constraint. Another constraint is the smallest separation of shells that can be resolved. This is given by $\Delta r = \pi/2\Delta k$ = 0.14 Å.[25] The addition of successive shells was tested for significance using the procedure of Joyner *et al.*[26] The k^3-weighted experimental and least-squares fitted EXAFS spectra of the aryl-mercury(II) compounds with the models/references are shown in Fig. 4; the corresponding Fourier transforms are shown in Fig. 5. The results of the least-squares fittings are contained in Table 1. Multiple scattering is not significant for the higher shells, indicating that the –Hg–O–Hg– groupings in each case are non-linear with angles <150° (ref. 24). This angular arrangement is supported by Hg···Hg distances in each sample less than *ca.* 4.1 Å (*i.e.* less than twice the Hg–O distance). Details for individual compounds are as follows.

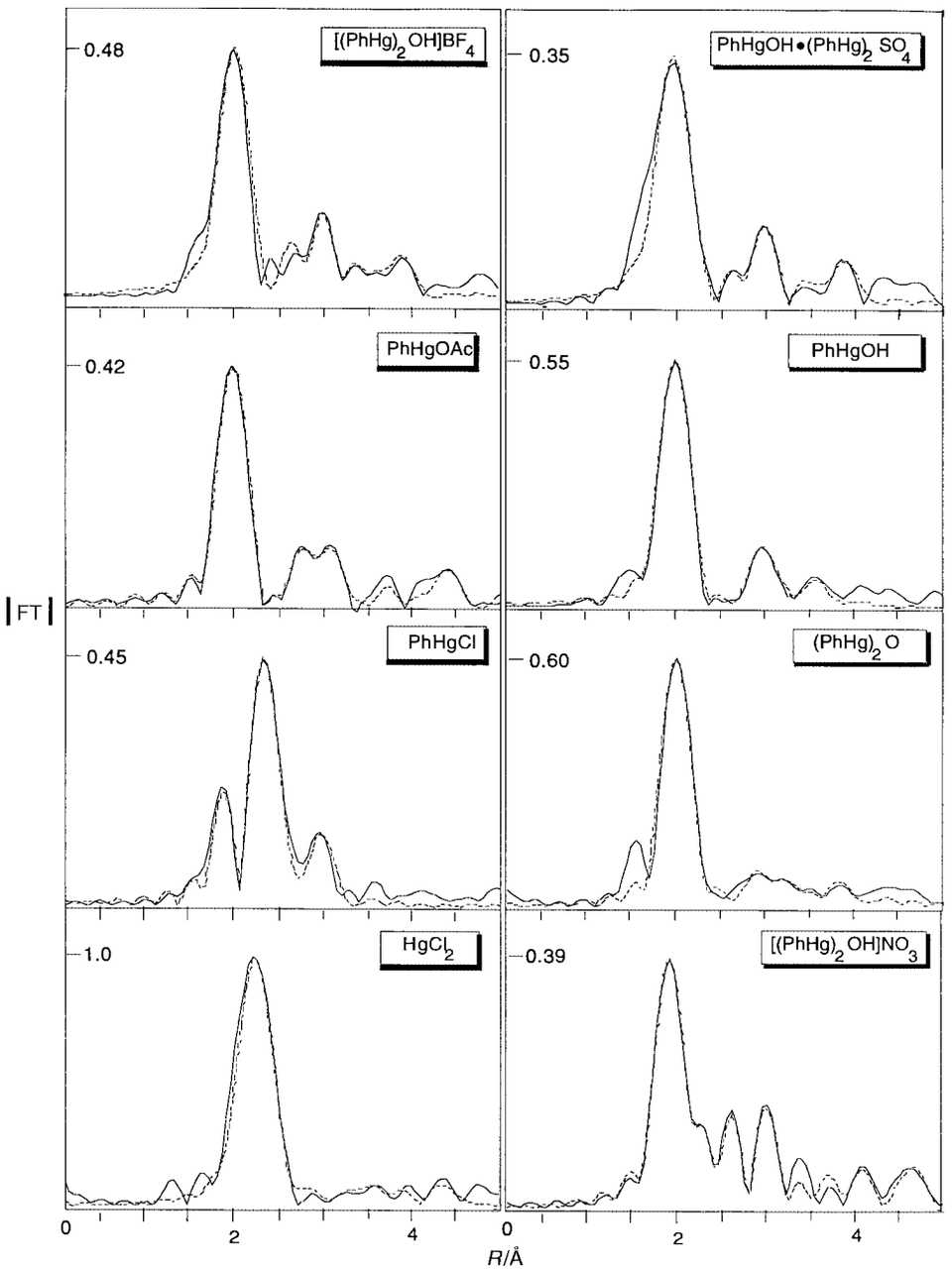

Fig. 5 The magnitude of the Fourier transform (FT) in arbitrary units. The solid line shows the FT of the experimental data and the broken line represents the FT of the calculated EXAFS.

$HgCl_2$. This compound was re-examined to provide a link to the earlier study.[10] A good fit was obtained using two Cl atoms at 2.29 Å. This compares with average Hg–Cl distances of 2.282 Å in the solid state structure determined by X-ray crystallography,[27] and is identical to the value found in the previous EXAFS study.[10] The Debye–Waller factors also agree with those of the earlier study, and have the low values that appear to be associated with heavy atom compounds.[10,28]

PhHgCl. This is a known structure, though the X-ray crystallography study was complicated by disorder of the phenyl rings.[16] The EXAFS results were readily modelled using one C at 2.05 Å (*ipso*-C), one Cl at 2.33 Å and two C atoms (*ortho*-C's) at 2.97 Å, which compares with crystallographic distances of 2.07, 2.33 and 3.00 Å respectively.[16] This shows that the EXAFS results for organomercury compounds do provide reliable parameters. In the crystal structure there are neighbouring Hg atoms at 4.3 and 4.6 Å, but the EXAFS FT trace shows little contribution from these so they were not included.

PhHgOAc. This was a model compound for C,O-bonded mercury. The X-ray crystal structure[17] shows the immediate environment at Hg consists of a C atom at 2.04 and an O atom at 2.08 Å. Since these were too similar to be distinguished by EXAFS they were included as two "average" N atoms, and refined to a distance of 2.05 Å, together with two *ortho*-C atoms at 2.94 Å. The shortest intermolecular distances are two Hg···O's and an Hg···C around 2.81 Å so these were also included to give a good fit to the data. The X-ray crystal structure shows a number of additional intermolecular Hg···O/C interactions in the 2.9–3.8 Å and nearest Hg···Hg neighbours are at 4.03 and 4.50 Å. Inclusion of these gave an excellent overall fit, but these longer range species would have been difficult to deduce in the absence of X-ray crystallography data.

$[(PhHg)_2OH][BF_4]\cdot H_2O$. This known structure[8] was expected to provide a good model for the other basic salts (see below). The EXAFS data were initially analysed using two "nitrogen" atoms at 2.05 Å and two carbon atoms at 3.05 Å

Table 1 EXAFS data

Sample	*N*	*r*/Å (EXAFS)[a]	*r*/Å (XRD)[b]	$2\sigma^2$/Å^2	E_o/eV	*R*%	FI(k^3)
Model compounds:							
$HgCl_2$	2(Cl)	2.290(1)	2.282	0.0071(3)	14.8(3)	24.8	1.1773
PhHgCl	1(Cl)	2.331(1)	2.33	0.0060(2)	19.0(2)	23.6	0.2291
	1(C)	2.045(2)	2.07	0.0022(4)			
	2(C)	2.973(1)	3.00	0.0053(35)			
PhHgOAc	2(C,O)	2.046(2)	2.06(av)	0.0085(3)	21.3(3)	22.0	0.1841
	3(C,2O)	2.805(23)	2.85(av)	0.023(2)			
	3(2C,O)	2.976(11)	3.0(av)	0.0189(26)			
	1(O)	3.202(52)	3.16	0.036(13)			
	4(C)	3.778(15)	3.80(av)	0.0309(42)			
	1(Hg)	4.085(24)	4.03	0.028(5)			
	1(Hg)	4.559(32)	4.50	0.030(7)			
$[(PhHg)_2OH]BF_4$	2 (O,C)	2.046(8)	2.03(av)	0.0050(35)	20.9(2)	23.7	0.2300
	2(F)	2.835(7)	3.01(av)	0.018(2)			
	2(C)	3.049(8)	2.97(av)	0.002(27)			
	1(F)	3.181(9)	3.23	0.0010(7)			
	1(Hg)	3.636(6)	3.64	0.014(11)			
Unknown structures:							
$(PhHg)_2O$	2(C,O)	2.017(2)		0.0041(3)	20.6(3)	22.4	0.2661
	2(C)	2.920(9)		0.0120(2)			
	2(C)	3.482(33)		0.0063(34)			
	1(Hg)	3.735(26)		0.022(9)			
PhHgOH	2(C,O)	2.017(1)		0.0050(2)	22.5(4)	17.7	0.1514
	2(C)	2.991(5)		0.0080(9)			
	1(Hg)	3.343(8)		0.0218(16)			
$PhHgOH·PhHgNO_3$	1(C)	1.999(1)		0.001(2)	18.6(2)	16.3	0.0946
	1(O)	2.195(2)		0.001(4)			
	1(O)	2.764(4)		0.0038(7)			
	2(C)	2.995(5)		0.0026(8)			
	1(O)	3.062(2)		0.0185(63)			
	1(Hg)	3.766(7)		0.0149(12)			
$PhHgOH·(PhHg)_2SO_4$	1(C)	1.999(7)		0.006(1)	20.8(6)	27.0	0.1932
	1(O)	2.131(14)		0.0099(42)			
	1(O)	2.766(16)		0.0165(36)			
	2(C)	2.999(10)		0.0063(16)			
	1(O)	3.174(19)		0.0126(46)			
	1(Hg)	3.584(9)		0.0178(17)			

[a] The standard deviation in the last significant digit as calculated by EXCURV90 is given in parentheses. However, note that such estimates of precision (which reflect statistical errors in the fitting) overestimate the accuracy. The estimated errors for distances are 0.01 Å at $r < 2.5$ Å with 20% accuracy for *N* and $2\sigma^2$, although the accuracy for these is increased by refinements using k^1 *vs.* k^3 weighting.[22] The fit index FI is defined in the text, and the residual index *R*% is given by: $(\sum_i [k^3(\chi_i^{exp} - \chi_i^{calc})]^2/\sum_i [k^3(\chi_i^{exp})]^2 \times 100$. [b] From X-ray crystal structure determinations (see text for individual references).

(corresponding to *ortho*-C's at 2.92 and 3.02 Å), and Hg···F interactions at 2.84 (×2) and 3.18 Å, close to those found in the crystal structure.[8] The data were also fitted to a model in which the composite two in-phase "nitrogen" atoms were split into their *ipso*-carbon and oxygen components. A slightly better fit ($R = 21.8\%$ *vs.* 23.7%) was obtained with carbon and oxygen distances of 2.00 and 2.06 Å, respectively. However the composite model was retained because the differences between these distances is less than the smallest separation of shells that can be resolved (see above). The Fourier transform of the difference spectrum showed that the strongest remaining feature was a peak at *ca.* 3.6 Å which clearly corresponds to the intramolecular Hg···Hg of 3.64 Å in the crystal structure, the full refinement exactly matching the crystallographic value. EXAFS does not directly provide angular information, but in this case the Hg–O–Hg angle can be readily calculated from the Hg–O and Hg···Hg distances to be 125°, which is in complete agreement with the X-ray crystallographic value of 126°. The concordance between the crystallographic and EXAFS results for this example lend support for the reliability of the parameters derived below for the compounds of previously unknown structure.

$(PhHg)_2O$. The structure of this compound is unknown, but chemical evidence suggests it is a discrete molecular species.[5] This is supported by an X-ray crystal structure determination of $[Ni(acac)_2(PhHgOHgPh)(Et_2O)]_2$, where the $(PhHg)_2O$ is bridging the two Ni atoms through the oxygen atom.[6] In this complexed form the Hg–O distance is 2.041(3) Å, the Hg–C 2.042(8) Å and the Hg–O–Hg angle is 119.4(3)°.

The EXAFS data for the free $(PhHg)_2O$ were initially fitted using two average C,O (*i.e.* N) atoms at 2.02 Å, and two *ortho* C atoms at 2.92 Å. A clear neighbouring Hg was evident at 3.74 Å and the fit was completed by two C atoms at 3.48 Å, presumably intermolecular interactions. All this is fully consistent with the molecular formulation. Again the Hg–O–Hg angle can be readily calculated from the Hg–O and Hg···Hg distances to be 135°. There appears to be no X-ray crystallographically characterised example of an uncomplexed $(RHg)_2O$ species,[29] so this is the first estimation of a simple Hg–O–Hg angle in an organo mercury oxide. The Hg–O–Hg angle of 135° for $(PhHg)_2O$ is wider than found in the Ni-complexed form, 119.4(3)°, and in the $[(PhHg)_2OH]^+$ cation, 125°, but this is expected because of the difference in the number of atoms attached to oxygen.

PhHgOH. As discussed in the introduction, the solid state structure of this is unknown. Several models were used to try to fit the EXAFS data, but the only viable one (which gave an excellent fit) was based on the $[(PhHg)_2OH]^+$ cation. This refined sensibly to give two "N" at 2.02 Å, two C at 2.99 Å and one Hg at 3.34 Å. Attempts to include an extra Hg (as in a $[(PhHg)_3O]^+$ cation for example) were rejected, so it is apparent

that "PhHgOH" is better formulated as $[(PhHg)_2OH]OH$. This is more consistent than a simple molecular formula with the complicated IR spectra reported earlier by Green.[7] The Hg···Hg and Hg–O distances allow the Hg–O–Hg angle to be calculated as approximately 112°, more acute than the 126° found for the same cation in the fluoroborate.

$PhHgOH·PhHgNO_3$. An unpublished X-ray crystal structure[9] indicated that this too contains the $[(PhHg)_2OH]^+$ cation, though further details are unavailable. The EXAFS FT (Fig. 5) shows much more pronounced structure than the other compounds in the series. For this compound it was necessary to include the *ipso*-carbon and the oxygen atom separately (rather than as averaged atoms as in the other examples) in order to reproduce the asymmetry in the dominant peak. This gave distances Hg–C 1.99 Å and Hg–O 2.19 Å. The difference in the Hg–C and Hg–O bond lengths is greater than the smallest separation of shells that can be resolved (see above). (EXAFS cannot unambiguously distinguish between a carbon and an oxygen atom, so the assignment to the two distances is based on the observation that in the crystal structures of compounds with a C_{aryl}–Hg–O linkage, the Hg–C distance is invariably shorter than the Hg–O distance, contrary to expectations from covalent radii). The two *ortho* carbon atoms were included at 2.99 Å as in the tetrafluoroborate model and it was also necessary to add extra oxygen atoms at 2.76 and 3.06 Å, which presumably represent mercury(II) interactions with adjacent nitrate anions (*cf.* the Hg···F interaction found in the X-ray crystal structure of the tetrafluoroborate described above and included in the EXAFS simulation). The remaining feature in the basic nitrate arises from the nearest Hg neighbour at 3.76 Å, and these all combined to give an excellent fit, based on a $[(PhHg)_2OH]^+$ cation. This leads to an Hg–O–Hg angle of 118°, intermediate between those of the other $[(PhHg)_2OH]^+$ cations discussed above.

$PhHgOH·(PhHg)_2SO_4$. This compound has an unknown structure. It may in fact have more than one crystalline form, given the markedly disparate melting points found in an earlier study[12] (270–280 °C) and in our study (152–158 °C) for ostensibly the same compound. This compound differs from the others examined in this study in that it contains a 2− anion and hence has a different stoichiometry. Two structures were examined, the first being the bis-oxonium cation $[(PhHg)_2OH]^+$ (as defined in the model compound $[(PhHg)_2OH][BF_4]·H_2O$, and found for the other basic salts), with the second being the tris-oxonium cation, $[(PhHg)_3O]^+$ which the ESMS data indicated was a feasible structure.

The EXAFS FT shown in Fig. 5 is evidently similar to that of the model compound $[(PhHg)_2OH][BF_4]·H_2O$ in its general features. However, it is clear that the first peak at *ca.* 2 Å is broader and more asymmetric than for the other compounds examined. This once again suggests partial resolution of the first shell carbon and oxygen atoms about mercury, as in the nitrate discussed above, and gave similar values (2.00 and 2.13 Å respectively). As well as the usual two *ortho* carbon atoms at 3.00 Å, there are additional oxygen atoms from an adjacent SO_4^{2-} at 2.77 and 3.17 Å. This leaves a feature assigned to one Hg atom at 3.58 Å , which in turn strongly suggests once more a $[(PhHg)_2OH]^+$ cation, with an Hg–O–Hg angle of 114°, similar to those found for the other examples.

Attempts to fit the EXAFS to the alternative structure, a tris-oxonium cation, $[(PhHg)_3O]^+$, by including two neighbouring Hg atoms were unsuccessful.

All this indicates that the basic sulfate also contains a bis-oxonium cation $[(PhHg)_2OH]^+$. However the stoichiometry of this compound (confirmed by elemental analysis) requires a formula of the type $[(PhHg)_2OH]^+$ $[PhHgSO_4]^-$ if the bis-oxonium is present. This in turn means that there will be more than one type of mercury in the lattice which will lead to overlapping EXAFS signals. This is consistent with the asymmetry of the dominant peak at *ca.* 2.0 Å, and with the suggestion of several Hg···Hg interactions around 4.0 Å. Because of this complexity and the limitations on the number of parameters that can be validly refined, further attempts at fitting this spectrum were not undertaken.

Conclusions

XAS provides reliable information for aryl–mercury compounds when single crystal samples cannot be obtained. The series examined in the present studies show that the Ph–Hg–O fragment is readily modelled using the O and *ipso*-C (combined and included as average N atoms when not resolved), and two *ortho*-C atoms. This grouping varies little, and can be subtracted from the total spectrum to highlight additional scattering atoms. This allows neighbouring Hg atoms to be readily identified as dominating second-shell contributions, and hence the extended geometry can be deduced.

In this way $(PhHg)_2O$ has been shown to be a molecular species with a Hg–O–Hg angle of 135°. The $[(PhHg)_2OH]^+$ cation, crystallographically characterised in $[(PhHg)_2OH][BF_4]·H_2O$, also occurs in "PhHgOH" which is better formulated as $[(PhHg)_2OH]OH$, and in the basic nitrate which is $[(PhHg)_2OH]NO_3$. It also appears to be present in the basic sulfate. For the four examples containing this cation, the Hg–O–Hg angle is calculated to be 125°, 112°, 118° and 114° respectively. This suggests some flexibility, possibly affected by longer range interactions of the Hg atoms with the counter-ions. The internal consistency of the results lends credence to the analysis of these structures using EXAFS, and we note that corresponding studies on other heavy-atom species have recently been reported for gold[28] and uranium.[30] A recent review describes other applications for XAS in coordination chemistry.[31] For mercury compounds, EXAFS is a useful complement to solid-state ^{199}Hg NMR techniques[32] for structure determination when single crystals suitable for X-ray diffraction are not available.

The ESMS studies show that the cation $[(PhHg)_3O]^+$ can exist, at least in solution, but we have been unable to find any evidence for it in any of the solid samples examined, in contrast to the methylmercury system where only the tris form $[(RHg)_3O]^+$ has been characterised in crystal structures.

Acknowledgements

Support from the Nansen Foundation and VISTA-Statoil (to D. G. N.) and the Norwegian Research Council (including a NATO Postdoctoral Fellowship to A. M.) is appreciated. Most of this work was carried out on the Swiss-Norwegian Beamline at the European Synchrotron Radiation Facility, Grenoble, France. Some of the samples were measured at the SRS, Daresbury Laboratory, using beamtime kindly made available by Dr G. Sankar. We thank the Norwegian University of Science and Technology and the Norwegian Research Council for grants to the SNBL Consortium. We also acknowledge the assistance of the SNBL Project Team (H. Emerich, P. Pattison and H. P. Weber). We are grateful to the Royal Society of Chemistry for a travel grant (to B. K. N.) to assist this study.

References

1 D. Grdenic and F. Zado, *J. Chem. Soc.*, 1962, 521
2 D. Grdenic and B. Kamenar, *Acta Crystallogr., Sect. A*, 1978, **34**, S127.
3 D. Grdenic and B. Markusic, *J. Chem. Soc.*, 1958, 2434; J. H. R. Clarke and L. A. Woodward, *Spectrochim. Acta*, 1967, **23A**, 2077; D. L. Rabenstein, C. A. Evans, M. C. Tourangeau and M. T. Fairhurst, *Anal. Chem.*, 1975, **47**, 338.
4 D. Breitinger and W. Morell, *Inorg. Nucl. Chem. Letters*, 1974, **10**, 409; W. Theil, F. Weller, J. Lorbeth and K. Dehnicke, *Z. Anorg.*

Allg. Chem., 1971, **381**, 57; A. Weiss, G. Nagorsen and A. Weiss, *Z. Anorg. Allg. Chem.*, 1953, **274**, 152; K. Aurivillius, *Acta Chem. Scand.*, 1954, **8**, 523; B. Kamenar, B. Kaitner and S. Pocev, *J. Chem. Soc., Dalton Trans.*, 1985, 2457.
5 A. J. Bloodworth, *J. Organomet. Chem.*, 1970, **23**, 27.
6 M. Doring, G. Hahn, M. Stoll and A. C. Wolski, *Organometallics*, 1997, **16**, 1879.
7 J. H. S. Green, *Spectrochim. Acta*, 1968, **24A**, 863.
8 B. K. Nicholson and A. J. Whitton, *J. Organomet. Chem.*, 1986, **306**, 139.
9 G. Grdenic, personal communication, 1984.
10 R. Åkesson, I. Persson, M. Sandstrom and U. Wahlgren, *Inorg. Chem.*, 1994, **33**, 3715.
11 J.-H. Choy, S.-J. Hwang and N.-G. Park, *J. Am. Chem. Soc.*, 1997, **119**, 1624.
12 L. R. Barlow and J. M. Davidson, *J. Chem. Soc.*, 1968, 1609.
13 L. J. Arnold, *J. Chem. Educ.*, 1992, **69**, 811.
14 *International Tables for X-Ray Crystallography*, Kynoch Press, Birmingham, 1962, vol. 3, p. 175.
15 EXCALIB, EXBACK and EXCURV90 programs, N. Binsted, J. W. Campbell, S. J. Gurman and P. C. Stephenson, SERC, Daresbury Laboratory, 1990.
16 J. Fayos, G. Artioli and R. Torres, *J. Crystallogr. Spectrosc. Res.*, 1993, **23**, 595.
17 B. Kamenar and M. Penavic, *Inorg. Chim. Acta*, 1972, **6**, 191; B. Kamenar, M. Penavic and A. Hergold-Brundic, *Croat. Chem. Acta*, 1984, **57**, 145.
18 W. H. Kampers, PhD Thesis, Eindhoven University of Technology, Eindhoven, 1988; F. W. H. Kampers, C. W. R. Engelen, J. H. C. Van Hooff and D. C. Koningsberger, *J. Phys. Chem.*, 1990, **94**, 8574.
19 A. Moen, D. G. Nicholson and M. Ronning, *J. Chem. Soc., Faraday Trans.*, 1995, **91**, 3189.
20 G. Lamble, A. Moen and D. G. Nicholson, *J. Chem. Soc., Faraday Trans.*, 1994, **90**, 2211.
21 L.-S. Kau, D. J. Spira-Solomon, J. E. Penner-Hahn, K. O. Hodgson and E. I. Solomon, *J. Am. Chem. Soc.*, 1987, **109**, 6433.
22 A. Moen, D. G. Nicholson, M. Ronning, G. M. Lamble, J.-F. Lee and H. Emerich, *J. Chem. Soc., Faraday Trans.*, 1997, **93**, 4071.
23 A. J. Bloodworth, *J. Chem. Soc. C*, 1970, 2051; A. J. Canty and J. W. Devereux, *Spectrochim. Acta*, 1980, **36A**, 495.
24 B. K. Teo, *EXAFS: Basic principles and data analysis*, Springer-Verlag, New York, 1986.
25 Report on the International Workshops on Standards and Criteria in XAFS in X-ray Absorption Fine Structure, ed. S. S. Hasnain, Ellis Horwood, Chichester, 1991, p. 751.
26 R. W. Joyner, K. J. Martin and P. Meehan, *J. Phys. Chem.*, 1987, **20**, 4005.
27 V. Subramanian and K. Seff, *Acta Crystallogr., Sect. B*, 1980, **36**, 2132.
28 P. Bishop, P. Marsh, A. K. Brisdon, B. J. Brisdon and M. F. Mahon, *J. Chem. Soc., Dalton Trans.*, 1998, 675.
29 Cambridge Crystallographic Database, April 1999 release.
30 W. W. Lukens, P. G. Allen, J. J. Bucher, N. M. Edelstein, E. A. Hudson, D. K. Shuh, T. Reich and R. A. Andersen, *Organometallics*, 1999, **18**, 1253.
31 J. E. Penner-Hahn, *Coord. Chem. Rev.*, 1999, **190**–**192**, 1101.
32 G. A. Bowmaker, R. K. Harris and S. W. Oh, *Coord. Chem. Rev.*, 1997, **167**, 49; G. A. Bowmaker, A. V. Churakov, R. K. Harris, J. A. K. Howard and D. C. Apperley, *Inorg. Chem.*, 1998, **37**, 1734.

Paper a906784a